Accelerated Sizing of a Power Split Electrified Powertrain

2020-01-0843

Accelerated sizing of a power split electrified powertrain

Pier Giuseppe Anselma
Politecnico di Torino / McMaster University

Atriya Biswas, Lucas Bruck, Saeed Amirfarhangi Bonab, Adam Lempert, and Joel Roeleveld
McMaster University

Krishna Madireddy, Omkar Rane, and Bryon Wasacz
FCA US LLC

Giovanni Belingardi
Politecnico di Torino

Ali Emadi
McMaster University

Abstract

Component sizing generally represents a demanding and time-consuming task in the development process of electrified powertrains. A couple of processes are available in literature for sizing the hybrid electric vehicle (HEV) components. These processes employ either time-consuming global optimization techniques like dynamic programming (DP) or near-optimal techniques that require iterative and uncertain tuning of evaluation parameters like the Pontryagin's minimum principle (PMP). Recently, a novel near-optimal technique has been devised for rapidly predicting the optimal fuel economy benchmark of design options for electrified powertrains. This method, named slope-weighted energy-based rapid control analysis (SERCA), has been demonstrated producing results comparable to DP, while limiting the associated computational time by near two orders of magnitude. In this paper, sizing parameters for a power split electrified powertrain are considered that include the internal combustion engine size, the two electric motor/generator sizes, the transmission ratios, and the final drive ratio. The SERCA approach is adopted to rapidly evaluate the fuel economy capabilities of each sizing option in various driving missions considering both type-approval drive cycles and real-world driving profiles. While screening out for optimal sizing options, the implemented methodology includes drivability criteria along with fuel economy potential. Obtained results will demonstrate the agility of the developed sizing tool in identifying optimal sizing options compared to state-of-the-art sizing tools for electrified powertrains.

Introduction

Improved fuel economy and customer acceptance constraints satisfaction at once is the strong suit of Hybrid Electric Vehicles (HEVs) [1]. Nevertheless, HEVs demonstrate a significantly complex design environment compared to both conventional vehicles (i.e. powered by an internal combustion engine (ICE) solely) and battery electric vehicles [2]. A challenging area indeed relates to the large variety of potential powertrain configurations (e.g. series, parallel, series-parallel, power split) and the several levels of hybridization (e.g. micro, mild, full, plug-in) [3]. The power-split configuration currently demonstrates the most successful powertrain architecture, being largely embedded in the actual production full HEVs [4]. Power split HEVs characterize by the employment of planetary gear (PG) sets, which are compact and can realize an electrically variable transmission (eVT) [5]. Advanced techniques are required to derive effective strategies for managing the power fluxes between the ICE and the electric power components in HEV design and sizing methodologies. The level of complexity for the interactions among HEV powertrain components proportionally increases with the hybridization level [6][7].

Off-line HEV supervisory control is particularly required in powertrain design processes to estimate the theoretical fuel economy capability of each potential design option over different pre-selected driving missions. In off-line HEV control, the overall driving mission profile is known a priori before running the simulation. The off-line energy management algorithm then optimizes the HEV powertrain operation in an attempt to minimize a defined cost function (usually represented by the fuel consumption) over the retained driving mission. The most known optimization-based off-line HEV supervisory controllers are represented by Dynamic Programming (DP) and the Pontryagin's Minimum Principle (PMP) [8]-[11]. Nevertheless, both these off-line HEV controllers present some drawbacks. DP can return the global optimal solution for the HEV off-line control problem, however it suffers from curse of dimensionality [12]. The PMP can achieve a sufficiently good approximation of the global optimal solution under certain conditions [13]. Its application for on-line HEV control, named equivalent fuel consumption minimization strategy (ECMS), could be straightforwardly implemented as on-board HEV supervisory controller. Nevertheless, in order to achieve charge balanced operation over the driving mission, the PMP necessitates the recursive tuning of a coefficient for the equivalent fuel consumption. In HEV design processes, the calibration of this coefficient should be repeated not only for each driving mission under study, but also for all the considered design options, thus compromising the flexibility

of the algorithm. Furthermore, straightforwardly reaching near-optimality in the solution of the HEV off-line control problem by means of the PMP is not always guaranteed [14]. To overcome these issues, a novel off-line HEV supervisory controller has recently been introduced under the name of slope-weighted energy-based rapid control analysis (SERCA). This algorithm has been developed ad hoc for rapidly solving the off-line HEV control problem while achieving a near-optimal solution in terms of fuel economy performance. Moreover, one feature of the SERCA algorithm concerns its flexible applicability to various HEV sizing options [15]. Nevertheless, when introduced, the SERCA algorithm has been applied for solving the HEV off-line control problem in a rapid and effective way exclusively for a single HEV powertrain layout. This paper therefore aims at further outlining the potential of the SERCA algorithm by integrating it in a dedicated sizing methodology for power split HEV powertrains. Particularly, the SERCA algorithm reveals an effective strategy to remarkably narrow the computational cost associated to the HEV sizing methodology.

Organization of this paper is as follows: the power split HEV powertrain configuration under study and the related modeling approach are firstly presented. Then, the SERCA algorithm is described as an effective sizing oriented HEV energy management approach. The accelerated sizing methodology for the retained HEV consequently finds illustration including evaluation criteria for both fuel economy and drivability performance. A successful case study for the power split HEV is then presented that considers as sizing parameters the ICE size, the electric motor/generator (MG) sizes, the transmission ratios and the final drive ratio. Conclusions will be finally drawn.

Power split HEV powertrain configuration

This section illustrates the HEV under study and the related modeling approach. The power split HEV powertrain configuration considered here particularly refers to the eFlite® hybrid transmission, introduced by Chrysler in 2017 being implemented in the 2017 Chrysler Pacifica minivan [16]. The eFlite® transmission diagram can be observed in Figure 1.

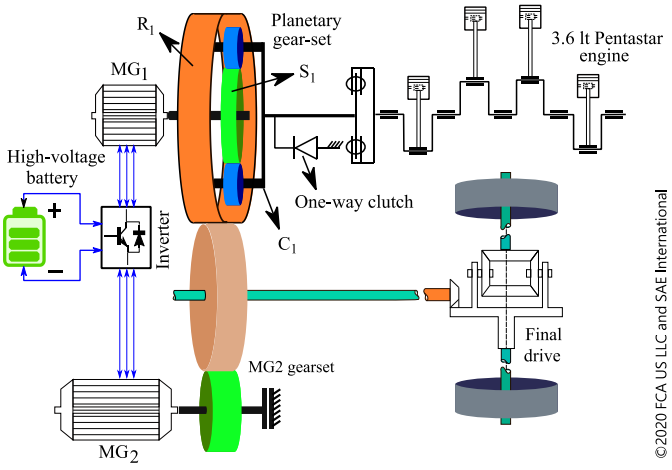

Figure 1. eFlite® transmission diagram.

eFlite® transmission driving operation

As shown in Figure 1, the eFlite® transmission embeds an ICE and two MGs. ICE, MG1 and transmission output shafts are kinematically constrained by means of a PG set being linked to the carrier, the sun gear and the ring gear, respectively. On the other hand, MG2 represents the main traction motor directly coupled to the output.

Two different driving modes can be operated by the eFlite® transmission, i.e. hybrid mode (HEV) and pure electric (EV) mode. In HEV mode, the PG set splits the ICE input into a mechanical driving path (through the ring gear) and an electrical generating path (through the sun gear). Particularly, MG1 reacts ICE power sending mechanical power out through the ring gear while generating electric power. Speed and torque of ICE and MG1 can be adjusted to optimize fuel efficiency and performance as an eVT feature. To enable EV operation, the eFlite® transmission embeds a one-way clutch (OWC) between ICE and PG sets. Since the OWC reacts torque from the PG carrier, MG1 can be used as well as traction motor in EV driving. In this case, the torque split between MG1 and MG2 can be varied to enhance electrical energy savings. During regenerative braking, only MG2 operates as generator to transform mechanical energy into electrical energy storable in the battery. More details about the eFlite® transmission operation can be found in [16].

HEV modeling approach

As commonly adopted in HEV design methodologies, a vehicle model constituted by analytical equations is simulated in a backward quasi-static approach with time step corresponding to 1 second [17]. Detailed modeling for the components of the considered HEV is presented as follows and implemented in MATLAB® software.

Road load and vehicle

The requested torque at the transmission output shaft can be evaluated backwardly at each time step using equation (1).

$$T_{out} = \left(F_{road} + m_{veh_{eq}} \cdot a\right) \cdot \frac{r_{dyn}}{i_{FD}} \quad (1)$$

F_{road} represents the road resistance forces (evaluated using experimental road load coefficients), $m_{veh_{eq}}$ is the vehicle equivalent mass evaluated at the wheel shaft considering the inertia of the powertrain rotating components (wheels, shafts, ICE and MGs), a represents the vehicle acceleration calculated from the vehicle speed in adjacent time points. r_{dyn} and i_{FD} are the wheel rolling radius and the final drive ratio, respectively.

Hybrid transaxle

Speed and torque equations can be written to model kinematics of the eFlite® hybrid transmission. Assuming a 1:1 ratio between the ring gear and the transmission output shaft gear in Figure 1, speed values for the power components (represented by ω) can be determined from the output speed value in equation (2).

$$\begin{gathered} \omega_{MG2} = \omega_{out} \cdot i_{MG2} \\ \omega_{MG1} \cdot S + \omega_{out} \cdot R = \omega_{ICE} \cdot (R + S) \end{gathered} \quad (2)$$

i_{MG2} refers to the MG2 transfer gearset (TG) ratio, while R and S represent the number of teeth for the ring gear and the sun gear of the PG set, respectively. ω_{MG2} is particularly constrained by the transmission output speed, while a 1 degree of freedom (DoF) relationship can be established between $\omega_{MG1}$and ω_{ICE} according to the PG kinematics. In EV driving, the OWC enables the same speed

equations for the power components while setting a null value of ω_{ICE}.

Concerning the values of torque for the power components (represented by T), equation (3) allows determining the values of T_{out} and T_{MG1} in HEV mode.

$$T_{out} = T_{ICE} \cdot \frac{R}{R+S} \cdot \eta_{TG}(\omega, T) + T_{MG2} \cdot i_{MG2} \cdot \eta_{PG}(\omega, T)$$
$$T_{MG1} = -T_{ICE} \cdot \frac{S}{R+S} \quad (3)$$

η_{GS} and η_{PG} denote the values of efficiency for the MG2 TG and the PG set. These can be represented by lookup tables with speed and torque as independent variables in order to improve the accuracy of the modeling approach. The retained hybrid transmission thus allows a 1 DoF relationship as well for the split between T_{ICE} and T_{MG2}. Following the torque relationship for a PG set, the MG1 is permanently set to produce a negative torque (i.e. work as a generator). In EV mode, a 1 DoF relationship can be established between T_{MG1} and T_{MG2}:

$$T_{out} = T_{MG1} \cdot \frac{R}{S} \cdot \eta_{TG}(\omega, T) + T_{MG2} \cdot i_{MG2} \cdot \eta_{PG}(\omega, T) \quad (4)$$

Power components

After the torque and speed values are established for the MGs, the requested battery output power P_{batt} can be evaluated using equation (5).

$$P_{batt} = \sum_{k=1}^{2} \omega_{MGk} \cdot T_{MGk} \cdot [\eta_{MGk}(\omega, T)]^{-sign(T_{MGk})} \quad (5)$$

η_{MG} represent the efficiency values of the MGs, determined according to empirical efficiency maps including inverter efficiencies with torque and speed as independent variables. An equivalent open circuit model is adopted here to simulate the behavior of the battery in equation (6).

$$\dot{SOC} = \frac{V_{OC} - \sqrt{{V_{OC}}^2 - 4 \cdot R_{IN} \cdot P_{batt}}}{2 \cdot R_{IN} \cdot Q_{batt}} \quad (6)$$

$\dot{SOC}$ represents the rate of battery State-of-Charge (SOC). V_{OC}, Q_{batt} and R_{IN} are the open-circuit voltage, the capacity and the internal resistance of the battery, respectively. Here, an approximation is adopted in considering R_{IN} and V_{OC} independent from the SoC as it has been demonstrated in literature that it is still possible to achieve a globally optimal solution with this hypothesis [18].
Finally, the rate of fuel consumption can be calculated as well from an empirical steady-state fuel flow map of the considered ICE with ω_{ICE} and T_{ICE} as independent variables.

Sizing oriented HEV energy management

This section aims at briefly describing the SERCA algorithm as an effective sizing oriented HEV off-line supervisory control strategy. This procedure is particularly required in order to estimate the fuel economy capability of sizing options for the HEV powertrain in CS operation over specific driving missions. The control variable set U related to the off-line HEV control problem for the eFlite® hybrid transmission is illustrated in equation (7).

$$U = \begin{Bmatrix} mode \\ U_{PS_{HEV/PS_{EV}}} \end{Bmatrix} \text{ with } U_{PS_{HEV}} = \begin{Bmatrix} \omega_{ICE} \\ T_{ICE} \end{Bmatrix}, \; U_{PS_{EV}} = \{T_{MG2}\} \quad (7)$$

U contains the operating mode selection (either HEV or EV) and the control variables related to the power split for the selected driving mode ($U_{PS_{HEV}}$ or $U_{PS_{EV}}$). In case the HEV mode is chosen, $U_{PS_{HEV}}$ includes the speed and torque values for the ICE. On the other hand, the torque value of MG2 needs determination for the $U_{PS_{EV}}$. In a backward simulation approach, the illustrated control variable set reveals enough as the remaining speed and torque values for the HEV powertrain components can be evaluated from the output speed and requested torque using equation (2) to equation (4).

The workflow of the SERCA algorithm is illustrated in Figure 2 and it can be divided into three main steps: the sub-problems exploration, the optimal operating hulls definition and the energy balance realization. The output information of SERCA is represented by the estimated fuel consumption (EFC) and the time series of control and state variables [15].

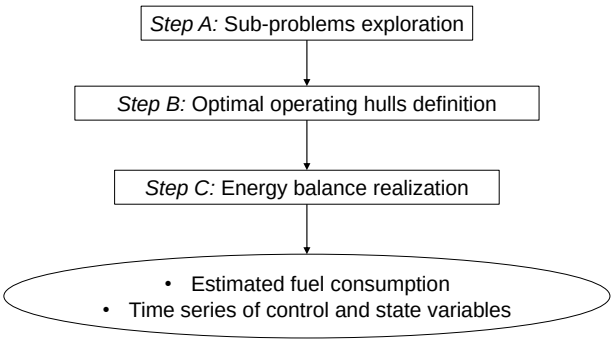

Figure 2. Operating steps of SERCA

A. *Sub-problems exploration*

In this paper, sub-problems that need resolution are represented by all the time instants of the driving mission under analysis. Particularly, a sub-problem is defined by values of current vehicle speed and desired acceleration, respectively. At this point, all the possible sub-solutions are explored for each sub-problem from the initial time instant of the retained driving mission to the final one.

The first sub-step involves the discretization of the control variable set. Concerning control variables related to speed and torque, these can be discretized according to retained resolution values and limiting their values within the correspondingly allowed operating regions, similarly to the DP procedure [12]. Each sub-solution is then represented by a specific set of values for the control variables. Sub-solutions are divided into HEV type and EV type according to the selected operating mode. At this point, a check is conducted for each sub-solution determining whether all the operating points of the power components (ICE, MGs, battery) are contained within the corresponding limits. Only the sub-solutions satisfying this feasibility check are maintained for the specific sub-problem, the rest of the sub-solutions are discarded.

The final part of this step aims at assessing the performance of all the feasible sub-solutions identified. EV sub-solutions only require the evaluation of $\dot{SOC}$ using equation (6), while HEV sub-solutions are defined by the corresponding fuel consumption (using the ICE fuel map) as well.

B. Optimal operating hulls definition

After all the possible sub-solutions are identified for the analyzed sub-problem (i.e. time instants of the driving mission), they can be assessed based on the EFC and the $\dot{SOC}$, as illustrated in Figure 3. The y axis particularly displays battery $\dot{SOC}$ with inverted sign, i.e. a positive y value means the battery is discharging and vice-versa.

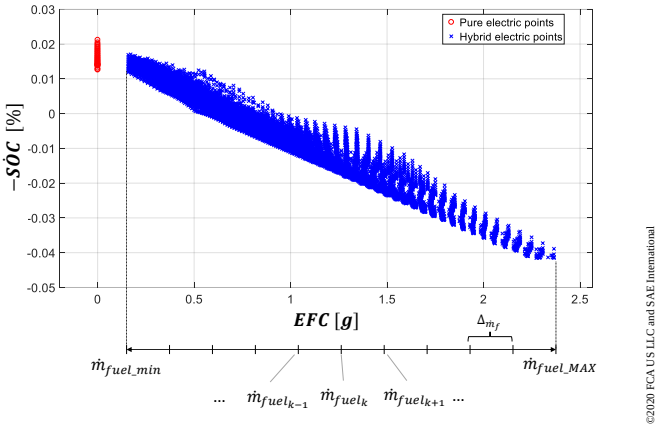

Figure 3. Example of sub-solutions comparison for a sub-problem.

The general descending trend of the hybrid electric sub-solutions cloud relates to the achievement of battery recharging through the gradual increase of fuel consumption. This plot can be translated in a sort of Pareto frontier for all the sub-solutions of the HEV powertrain in the specific sub-problem. The sub-solutions at the lower edge of the point cloud thus represent the optimal ones, since they present the upmost proportion between SOC increase and corresponding amount of fuel consumed. These points form an optimal hull and they should consequently be retained for eventual hybrid operation when tentatively pursuing the global optimal EFC solution in the driving mission analyzed. A similar approach is adopted in the ECMS to define an optimal ICE operating line [18], nevertheless the SERCA deals with discrete operating points rather than continuous variables. In order to identify and store the optimal hull of sub-solutions, the fuel consumption interval $[\dot{m}_{fuel\_min}, \dot{m}_{fuel\_MAX}]$ for the sub-problem in Figure 3 is discretized in a certain number of equidistant points $\dot{m}_{fuel_k}$. Subsequently, the optimal sub-solution corresponding to each span of the fuel consumption interval is identified and stored in a discretized optimal hull. Finally, the slope value is evaluated for each sub-solution of the identified optimal discrete hull. Considering the slope θ between adjacent sub-solutions of the discrete hull (e.g. point k and point $k-1$) represents the highlight of the SERCA algorithm as performed in equation (8).

$$\theta(k-1,k) = \frac{\Delta \dot{SOC}}{\Delta \dot{m}_{fuel}} = \frac{\dot{SOC}(k) - \dot{SOC}(k-1)}{\dot{m}_{fuel}(k) - \dot{m}_{fuel}(k-1)} \quad (8)$$

The slope relates to the ratio between the charged battery energy and the correspondingly consumed fuel when progressively shifting towards sub-solutions of the optimal hull with increased fuel consumption. As regards the optimal sub-solution corresponding to the minimum fuel consumption $\dot{m}_{fuel\_min}$, its slope can be directly calculated with reference to the optimal pure electric sub-solution.

Once this procedure is completed for all the sub-problems of the considered driving mission, the analysis results can be saved in a variable with the structure illustrated in Table 1. For the sub-solutions of the optimal hull, u represents the control variables (i.e. speed and torque of power components), while x contains the correspondent state variables and can be described in equation (9) for the generic sub-solution k of the discretized optimal hull for the sub-problem i.

$$\begin{aligned} u_{1|_{i,k}} &= \theta_i(k-1,k) \\ u_{2|_{i,k}} &= \dot{SOC}_i(k) - \dot{SOC}_i(k-1) \\ u_{3|_{i,k}} &= \dot{m}_{fuel_i}(k) - \dot{m}_{fuel_i}(k-1) \end{aligned} \quad (9)$$

An additional variable is created including the control and state variables of the optimal pure electric sub-solution for each sub-problem. It should be noted that only the sub-solutions illustrated in Table 1 are stored in the software memory for the driving mission, whereas in DP all the possible sub-solutions of each sub-problem need to be stored in memory, thus reducing the computational efficiency.

Table 1. Stored variable for the driving mission

Driving mission sub-problems	Optimal hybrid sub-solution #1	…	Optimal hybrid sub-solution *k*	…	Optimal hybrid sub-solution *N*
…	…	…	…	…	…
i-1	$u_{i-1,1}$, $x_{i-1,1}$	…	$u_{i-1,k}$, $x_{i-1,k}$	…	$u_{i-1,N}$, $x_{i-1,N}$
i	$u_{i,1}$, $x_{i,1}$	…	$u_{i,k}$, $x_{i,k}$	…	$u_{i,N}$, $x_{i,N}$
i+1	$u_{i+1,1}$, $x_{i+1,1}$	…	$u_{i+1,k}$, $x_{i+1,k}$	…	$u_{i+1,N}$, $x_{i+1,N}$
…	..	…	…	…	…

C. Energy balance realization

The final step of the SERCA algorithm addresses the solution of the HEV off-line control problem for the considered driving mission. This procedure has been derived by the energy-balance realization approach originally employed in the power-weighted efficiency analysis for rapid sizing (PEARS) algorithm [19]. The corresponding workflow is shown in Figure 4 and detailed as follows:

Step C.1: First it is assumed that the powertrain operates in EV mode only. Particularly, in the Pareto frontier of Figure 3 the optimal EV sub-solution is retained for each time instant of the driving mission. If EV operation is not allowed (e.g. due to power constraints), the optimal HEV sub-solutions corresponding to $\dot{m}_{fuel\_min}$ is retained. The required electrical energy E_{EV} is then given by the sum of the battery energy consumption at each time instant. E_{EV} can thus be interpreted as the total amount of electrical energy needed to complete the driving mission in electric operation only. The overall fuel consumption m_{fuel_TOT} is set to 0.

Step C.2: Looking at the first column of the variable shown in Table 1, the sub-problem i with the highest value of slope ($|\theta_i| = |\theta_{MAX}|$) is selected for hybrid operation. The values of control variables corresponding to the identified HEV sub-solution are then set to operate in the instant i.

Step C.3: The variables related to the overall driving mission are updated in Equation (10). Particularly, the overall value of required electrical energy is reduced by the value of charged battery energy in correspondence of the selected HEV sub-solution for the sub-problem i. At the same time, the global fuel consumption m_{fuel_TOT} is

increased according to the HEV sub-solution selected at time instant *i*.

$$\begin{aligned} \mathrm{E}_{EV} &= \mathrm{E}_{EV} + u_{2|_{i,1}} \\ \mathrm{m}_{fuel\_TOT} &= \mathrm{m}_{fuel\_TOT} + u_{3|_{i,1}} \end{aligned} \quad (10)$$

Finally, control and state variables corresponding to the selected driving mission point *i* are updated in Table 1. Particularly, the content of the first column of row *i* is deleted and the vector containing the remaining columns is shifted one position leftwards.

Step C.4: A check is performed for the charge balanced operation being achieved. This relates to the current value of E_{EV} being negative or null. In case this condition is not satisfied, steps C.2 and C.3 are iterated. Alternatively, the procedure is completed and the corresponding EFC is obtained by means of m_{fuel_TOT}, together with the time series of control and state variables over the analyzed driving mission.

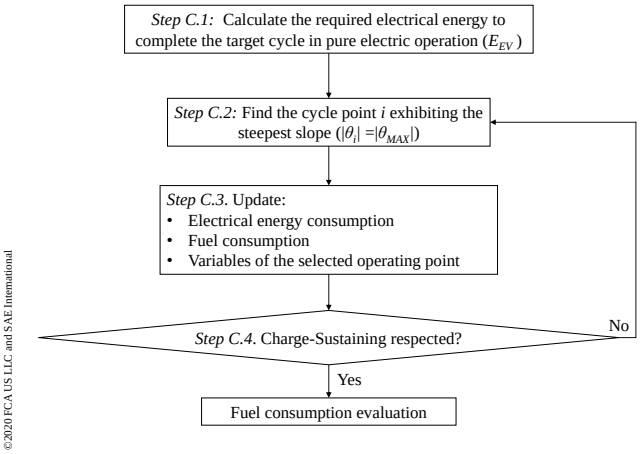

Figure 4. Flowchart of step C of SERCA.

Similarly to the PEARS algorithm, a minimization process for the number of ICE starts can be realized while preserving the proximity with the global optimal solution. This procedure can be implemented by integrating a coefficient that in step C.2 decides whether to give priority to the points adjacent to the previously considered one for the replacement process. This approach is described in further details in [20][21].

Accelerated sizing methodology

This section aims at describing the accelerated sizing methodology developed in this work for the power split HEV powertrain under consideration. Retained sizing parameters include the ICE size, the MG1 size, the MG2 size, the PG ratio, the MG2 TG ratio and the final drive ratio. A complete workflow of the sizing methodology is illustrated in Figure 5. In general, at each sizing iteration, current values of sizing parameters under analysis are initially set. A check is consequently conducted to verify that the HEV powertrain embedded with the specific sizing candidate comply with some gradeability and drivability requirements. In case the sizing candidate reveals successful, an evaluation of its performance is carried out based on some EFC and drivability criteria. The sizing candidate under analysis is discarded in case it does not meet all the criteria imposed at *Step 1*, and a new set of sizing parameters is selected at the next sizing iteration. This procedure is iterated until all the sizing candidates have been analyzed, and the overall sizing results are then assessed. In general, a brute force algorithm is adopted here to explore the sizing space. This reveals one of the most flexible approaches to exhaustively compare the sizing options and to handle different types of sizing variables (i.e. both continuous and discrete). Indeed, different power components are analyzed in this paper by considering their specific empirical operational map, rather than simply scaling one selected map per component type solely. Specific criteria for assessing gradeability, drivability and EFC of sizing candidates will be detailed in the follow-up of this section.

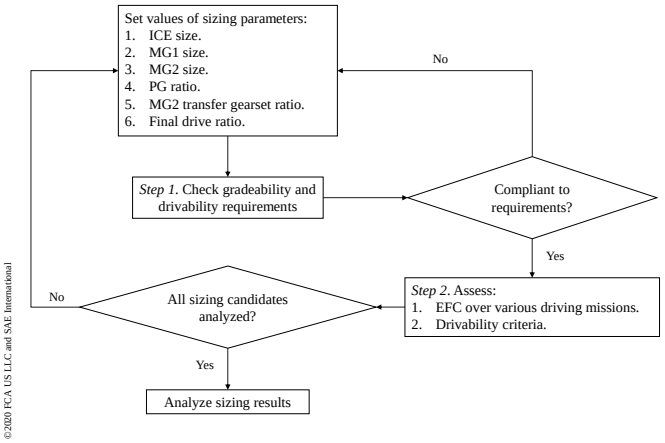

Figure 5. Workflow of the sizing methodology.

Gradeability and drivability requirements

Some mandatory gradeability and drivability requirements are considered in this paper for the sizing candidates under analysis. Table 2 illustrates the retained criteria from [22].

Table 2. Gradeability and drivability requirements at Step 1

Test #	Road slope	Requirement
1	30 %	Perform a standing start
2	0 %	Maintain vehicle speed at 150 km/h
3	14 %	Maintain vehicle speed at 80 km/h
4	7.2 %	Capability to charge-sustain the battery at 130 km/h

All the listed criteria are simulated using the vehicle model described at Section 2 of this paper. Test #1 requires the HEV to achieve a standing start considering a road slope of 30 %. Tests #2 and #3 demand the HEV powertrain to compensate the resistive forces at 150 km/h and 80 km/h with a constant road slope of 0 % and 14 %, respectively. Finally, Test #4 aims at ensuring that the HEV powertrain can eventually charge sustain the battery when travelling at 130 km/h on a road with 7.2 % slope.

In the implemented methodology, only the sizing candidates complying with the illustrated gradeability and drivability requirements are considered for further evaluation. Their assessment is particularly carried out based on two aspects, i.e. drivability and fuel economy.

Assessment of sizing options: drivability criteria

Design options satisfying the requirements illustrated above are assessed according to drivability criteria represented by "full throttle" maneuvers in this paper. The operating mode (i.e. pure electric or hybrid) capable of providing the highest tractive power to the wheels is selected at each time instant. A limitation is moreover considered in the deliverable tractive torque to the wheels accounting for tire adherence limits. A longitudinal tire behavior model based on the Pacejka's formulation with the maximum allowed tire longitudinal force depending on the corresponding vertical load is particularly considered [23]. During numerical simulations considering the illustrated vehicle model implemented in Simulink®, the amount of time required to complete each maneuver is evaluated. Here, four different acceleration maneuvers on a flat road are retained and associated to the following values of initial and final speed:

- 0 – 30 km/h
- 30 – 60 km/h
- 60 – 100 km/h
- 100 – 130 km/h

Assessment of sizing options: fuel economy

Other than drivability, the second important feature of the assessment of sizing options relates to fuel economy. In this paper, different driving missions are considered for the power split HEV. Then, the fuel economy capability of each sizing option in each considered driving mission is carried out in CS mode according to the SERCA algorithm. The following driving missions are particularly analyzed here:

- Urban dynamometer driving schedule (UDDS)
- Highway fuel economy test (HWFET)
- Worldwide harmonized light-vehicle test procedure (WLTP)
- US06 Supplemental Federal Test Procedure (US06)
- Real-world driving mission #1 (RWD#1)
- Real-world driving mission #2 (RWD#2)
- Real-world driving mission #3 (RWD#3)

The last three missions refer to real-world journeys for which the vehicle speed and altitude values were recorded by means of a global positioning system (GPS). Obtained time series for the recorded signals of the three missions are illustrated in Figure 6 along with the US06. RWD#1 and RWD#2 particularly represent downhill and uphill driving conditions, respectively, accompanied by some extra-urban and highway driving. They were recorded in Langhe, a hilly area in Piedmont, northern Italy. RWD#3 considers urban driving conditions solely and it was recorded in the city of Torino, northern Italy. Statistics for the retained real-world driving missions are reported in Table 3 where D, T, v, a and θ refer to distance, time, speed, acceleration and slope, respectively.

Table 3. Statistics for real-world driving missions.

	D [km]	T [s]	V_{avg} [km/h]	a_{avg+} [m/s^2]	a_{avg-} [m/s^2]	θ_{avg+} [%]	θ_{avg-} [%]
RWD #1	15.60	1357	41.38	0.44	-0.54	7.61	-4.82
RWD #2	17.87	936	68.74	0.62	-0.62	3.64	-1.60
RWD #3	4.14	901	16.53	0.62	-0.62	2.23	-3.01

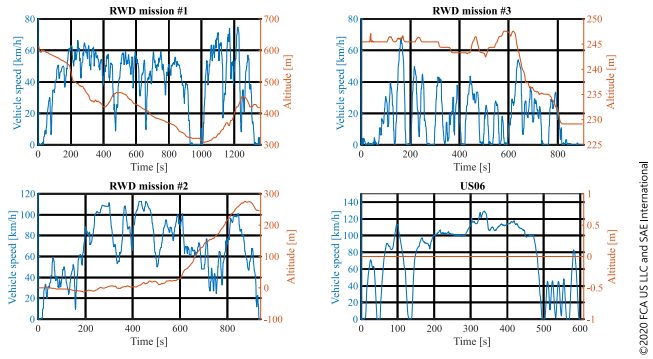

Figure 6. Profiles of real-world driving missions.

Results

This section aims at illustrating results obtained from the described sizing methodology for power split HEV powertrains. The selected vehicle in this paper relates to the 2017 Chrysler Pacifica minivan as it embeds the eFlite® hybrid transmission. Corresponding vehicle data are retained from [16] and illustrated in Table 4.

Table 4. Pacifica hybrid data.

Component	Parameter	Value
Vehicle	Mass	2381 Kg
	Wheel dynamic radius	0.348 m
Engine	Displacement	3.6 L
	Maximum power	164 kW
	Maximum torque	319 Nm
Transmission	PG ratio (R:S)	3.15
	MG2 TG ratio	2.59
	Final drive ratio	3.59
MG1	Maximum power	63 kW
	Maximum speed	12500 rpm

	Maximum torque	125 Nm
MG2	Maximum power	85 kW
	Maximum speed	12500 rpm
	Maximum torque	315 Nm

Different sizing options are then evaluated in an attempt to ameliorate the performance of the current HEV layout under study. In this paper, sizing parameters relate to the choice on the specific embedded ICE, MG1 and MG2, and the value of the three transmission ratios (PG ratio, MG2 TG ratio, final drive ratio). Considered parameters for the sizing candidates in this work are reported in Table 5 in the Appendix. Three different ICEs, three different values for each transmission ratio and five different components for both MG1 and MG2 are particularly considered. This leads to a sizing space comprising totally 2025 possibilities which are derived by all the possible combinations of sizing parameter values.

In the assessment of the sizing candidates, the crucial step in terms of computational cost relates to the evaluation of the EFC. As example, retaining the 7 driving missions illustrated above for each of the 2025 sizing possibilities would lead to analyze 14175 driving missions. In case DP was used as off-line HEV controllers to evaluate the EFC, the computational time required to process each driving mission for the considered HEV powertrain layout would be around 357 minutes on a desktop computer with Intel Core i7-8700 (3.2 GHz) and 32 GB of RAM [15]. This would lead to an amount of computational time required to complete the overall sizing procedure of around 3514 days (i.e. around 10 years). To avoid the mentioned course of dimensionality, two expedients can be adopted. The first one considers screening out feasible designs in terms of drivability and gradeability requirements before conducting the assessment in terms of EFC and acceleration performance, as illustrated in Figure 5. This allows to rapidly discard sizing candidates whose drivability performance is not satisfactory. For the considered sizing parameters, according to the implemented drivability requirements of Table 2, only 320 feasible sizing candidates are indeed identified and further evaluated. The second suggested procedure to reduce the computational cost and accelerate the completion of the sizing methodology refers to the adoption of the SERCA algorithm instead of DP for assessing the EFC of sizing candidates. Evaluating the EFC for a driving mission using SERCA requires indeed on average around 5 minutes for the same computational power reported above. This corresponds to around 187 hours required to analyze each of the 7 retained driving missions for each of the 320 identified feasible sizing candidates.

Once the methodology is completed, the analysis of obtained sizing results is carried out based on 5 parameters:

- Environmental Protection Agency (EPA) fuel economy
- WLTP fuel economy
- RWD fuel economy
- 0 – 100 km/h acceleration
- Averaged acceleration

Where the EPA fuel economy refers to the EPA's fuel economy procedure of considering 55 % weight on the UDDS and 45 % on the HWFET [24]. The WLTP fuel economy analyzes the WLTP alone, while the RWD fuel economy considers an average of the values of EFC (in l/100 km) for the US06 procedure and the three RWD cycles. The 0-100 km/h acceleration refers to the time necessary for the HEV powertrain sizing candidate to complete the corresponding maneuver, while the averaged acceleration index considers an average of the time spans requested to complete each of the four acceleration maneuvers reported in the previous section.

A ranking of all the feasible sizing candidates is then established for each of the five parameters described above. The optimal sizing candidates can be finally identified by averaging each of the five obtained rankings. In this paper, the three best sizing candidates are considered both for petrol-fueled engine HEVs ('OptGsl#1','OptGsl#2', OptGsl#3') and for diesel oil-fueled engine HEVs ('OptDsl#1','OptDsl#2', OptDsl#3'). The HEV sizing candidate embedding the components of the actual eFlite® hybrid transmission is considered as well for benchmarking the sizing candidates. Parameters and performance results for the identified optimal sizing candidates are reported in Table 6 in the Appendix, while Figure 7 shows a comparison of the sizing candidates with percentage performance data normalized according to the eFlite® ones.

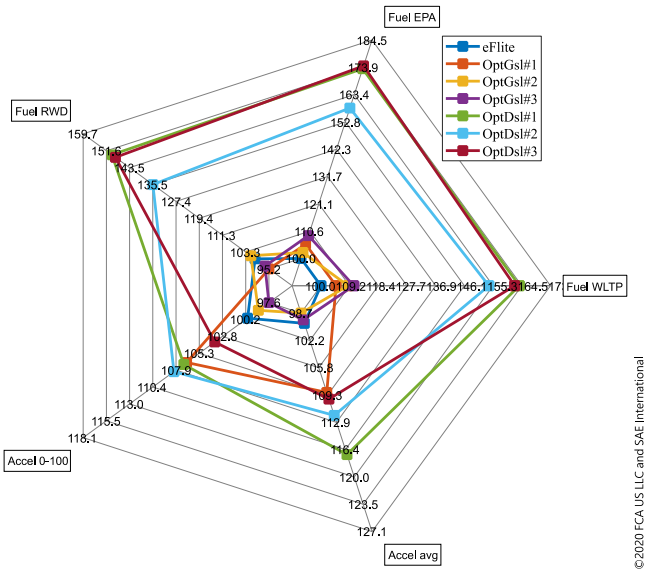

Figure 7. Results for the HEV sizing methodology.

The illustrated sizing methodology allows determining optimal sizing candidates according to the reported criteria. According to obtained results, overall improving the current eFlite® hybrid transmission performance does not seem possible by embedding a gasoline-fueled ICE. As example, 'OptGsl#1' ameliorates eFlite® by 5.22 %, 4.64 % and 6.29 % in terms of EPA EFC, WLTP EFC and 0-100 km/h acceleration, nevertheless its corresponding performance in terms of RWD EFC is 5.04 % worse than the eFlite® one. This might represent a disadvantage from the consumers' perspective. On the other hand, 'OptGsl#2' and 'OptGsl#3' could both ameliorate type-approval EFC with respect to eFlite® (-2.26 % and -8.13 % respectively for the EPA EFC, -8.06 % and -9.57 % respectively for the WLTP EFC). However, their corresponding drivability performance reveals worsening (+1.20 % and +2.41 % respectively for the 0-100 km/h acceleration time). Overall improvements not achievable through a gasoline-powered ICE could however be

overcome by installing a diesel oil-fueled ICE on the HEV. As a matter of fact, all the three optimal sizing candidates embedding a diesel ICE demonstrate a great potential for the general improvement of the HEV performance. 'OptDsl#1', 'OptDsl#2' and 'OptDsl#3' could indeed improve the eFlite® both in terms of EPA EFC (-42.34 %, -36.78 % and -42.70% respectively), WLTP EFC (-38.40%, -35.05 % and -38.38 % respectively), RWD EFC (-33.18 %, -26.18 % and -32.64 % respectively) and 0-100 km/h acceleration capability (-6.56 %, -7.50 % and -3.48% respectively). These results suggest that a downsized (i.e. 3.0 L instead of 3.6 L) diesel ICE, combined a properly sized MGs and transmission ratios, can achieve remarkably improved results compared to the current gasoline ICE benchmark. Further analysis would be necessary to assess the economic feasibility of these changes in current production HEVs.

Conclusions

This paper illustrates an accelerated sizing methodology for a power split HEV powertrain. The power split HEV under study is initially described and its numerical model is introduced. Then, the SERCA algorithm is presented as an effective numerical tool to rapidly assess the fuel economy capability of each sizing candidate by efficiently solving the HEV off-line control problem over selected driving missions. The overall sizing methodology finds then description including the mandatory satisfaction of selected drivability and acceleration requirements, and the evaluation according to fuel economy and drivability criteria. A case study is then presented considering the sizing process for the power split HEV powertrain. Retained sizing parameters include the ICE size and type, the MG1 size, the MG2 size, the PG ratio, the TG ratio and the FD ratio. Different sizing options can be generated as combinations of the swept sizing parameters. The set of components related to the current eFlite® hybrid transmission is retained as well, and its performance is considered as benchmark for the sizing options.

By means of the SERCA algorithm, it becomes thus possible to estimate the fuel economy for 320 different sizing options over 7 different selected driving missions including both type-approval cycles and RWD in approximately 187 hours. Obtained results suggest that an absolute improvement of the current state-of-the-art eFlite® hybrid transmission performance cannot be achieved using the considered gasoline-fueled ICEs. Indeed, improvements in terms of type-approval fuel economy can be accomplished only by worsening either the RWD EFC or the drivability performance. On the other hand, apparently an eFlite® hybrid transmission embedding a diesel oil-fueled ICE would remarkably ameliorate the performance of the current HEV layout both in terms of EFC and drivability performance. Improvements amounting at up to around 40 % could particularly be achieved in terms of fuel economy.

Future work could aim at evaluating the sizing candidates more accurately. Particularly, a more detailed HEV modelling approach could be adopted considering as example higher order dynamics of the transmission [25] and the after-treatment system. Moreover, further evaluation criteria could be implemented for the sizing methodology (e.g. operative cost, retail price). Finally, integrating the design and calibration of the on-board real-time hybrid supervisory control in the sizing methodology could be considered [26].

References

1. A. Emadi, "Transportation 2.0", *IEEE Power and Energy Magazine*, 9(4), pp. 18-29, 2011.
2. P.G. Anselma, G. Belingardi, "Comparing battery electric vehicle powertrains through rapid component sizing", *Int. J. Electric and Hybrid Vehicles*, vol.11, no.1, pp. 36-58, 2019.
3. P.G. Anselma, G. Belingardi, "Next generation HEV powertrain design tools: roadmap and challenges," *SAE Technical Paper* 2019-01-2602, 2019.
4. Y. Yang, K. Arshad-Ali, J. Roeleveld, A. Emadi, "State-of-the-art electrified powertrains – hybrid, plug-in, and electric vehicles", *Int. J. Powertrains*, 2016; 5(1), pp. 1-29.
5. A. Emadi, K. Rajashekara, S. Williamson, S. Lukic, "Topological Overview of Hybrid Electric and Fuel Cell Vehicular Power System Architectures and Configurations," *IEEE Transactions on Vehicular Technology*, vol. 54, no. 3, pp. 763-770, 2005.
6. S. M. Lukic and A. Emadi, "Effects of drivetrain hybridization on fuel economy and dynamic performances of parallel hybrid electric vehicles," *IEEE Transactions on Vehicular Technology*, vol. 53, pp. 385–389, 2004.
7. I. J. Albert, E. Kahrimanovic, and A. Emadi, "Diesel Sport Utility Vehicles With Hybrid Electric Drive Trains," *IEEE Transactions on Vehicular Technology*, vol. 53, No. 4 pp. 1247–1256, 2004.
8. S. G. Wirasingha and A. Emadi, "Classification and Review of Control Strategies for Plug-In Hybrid Electric Vehicles," *IEEE Transactions on Vehicular Technology*, vol. 60, no. 1, pp. 111-122, 2011.
9. A. Biswas and A. Emadi, "Energy Management Systems for Electrified Powertrains: State-of-the-Art Review and Future Trends," *IEEE Transactions on Vehicular Technology*, vol. 68, no. 7, pp. 6453-6467, 2019.
10. Bruck, L., Emadi, A. and Divakarla, K.P. "A review of the relevance of driving condition mapping and vehicle simulation for energy management system design', *Int. J. Powertrains*, Vol. 8, No. 3, pp.224–251, 2019.
11. G. Belingardi, P.G. Anselma, M. Demic, "Optimization-based controllers for hybrid electric vehicles", *Mobility & Vehicle Mechanics*, vol. 44, no. 3, pp. 53-67, 2018.
12. J. Lempert, B. Vadala, K. Arshad-Aliy, J. Roeleveld and A. Emadi, "Practical Considerations for the Implementation of Dynamic Programming for HEV Powertrains," *2018 IEEE Transportation Electrification Conference and Expo (ITEC)*, Long Beach, CA, 2018, pp. 755-760.
13. Kim, N., Rousseau, A., "Sufficient conditions of optimal control based on Pontryagin's minimum principle for use in hybrid electric vehicles", *Proceedings of the Institution of Mechanical Engineers, Part D: Journal of Automobile Engineering*, 226(9), 1160–1170, 2012.
14. Dabadie, J., Sciarretta, A., Font, G., and Le Berr, F., "Automatic Generation of Online Optimal Energy Management Strategies for Hybrid Powertrain Simulation," *SAE Technical Paper* 2017-24-0173, 2017.
15. P. G. Anselma, Y. Huo, J. Roeleveld, G. Belingardi and A. Emadi, "Slope-Weighted Energy-Based Rapid Control Analysis for Hybrid Electric Vehicles," in *IEEE Transactions on Vehicular Technology*, vol. 68, no. 5, pp. 4458-4466, 2019.
16. Pittel, M. and Martin, D., "eFlite® Dedicated Hybrid Transmission for Chrysler Pacifica," *SAE Technical Paper* 2018-01-0396, 2018.
17. P.G. Anselma, Y. Huo, J. Roeleveld, A. Emadi, G. Belingardi, "Rapid Optimal Design of a Multimode Power Split Hybrid Electric Vehicle Transmission", *Proceedings of the Institution of Mechanical Engineers, Part D: Journal of Automobile Engineering*, vol. 233, no. 3, pp. 740-762, 2019.
18. N. Kim, S. Cha and H. Peng, "Optimal Control of Hybrid Electric Vehicles Based on Pontryagin's Minimum Principle,"

in *IEEE Transactions on Control Systems Technology*, vol. 19, no. 5, pp. 1279-1287, 2011.
19. X. Zhang, H. Peng, J. Sun, “A near-optimal power management strategy for rapid component sizing of power-split hybrid vehicles with multiple operating modes,” in *American Control Conference (ACC)*, 2013, pp.5972-5977.
20. P.G. Anselma, Y. Huo, E. Amin, J. Roeleveld, A. Emadi, G. Belingardi, “Mode-shifting Minimization in a Power Management Strategy for Rapid Component Sizing of Multimode Power-split Hybrid Vehicles,” *SAE Technical Paper* 2018-01-1018, 2018.
21. G. Buccoliero, P. G. Anselma, S. Amirfarhangi Bonab, G. Belingardi and A. Emadi, "A New Energy Management Strategy for Multimode Power Split Hybrid Electric Vehicles," in *IEEE Transactions on Vehicular Technology*, in press, 2020.
22. P.G. Anselma, G. Belingardi, A. Falai, C. Maino, F. Miretti, D. Misul, E. Spessa, “Comparing Parallel Hybrid Electric Vehicle Powertrains for Real-world Driving”, *2019 AEIT International Conference of Electrical and Electronic Technologies for Automotive*, Torino, Italy, 2019, pp. 1-6.
23. Bakker, E., Pacejka, H., and Lidner, L., "A New Tire Model with an Application in Vehicle Dynamics Studies," *SAE Technical Paper* 890087, 1989.
24. Gasoline Vehicles: Learn More About the New Label, Environmental Protection Agency website [Online]. Available: https://www.fueleconomy.gov/feg/label/learn-more-gasoline-label.shtml
25. P.G. Anselma, A. Biswas, J. Roeleveld, G. Belingardi, A. Emadi, “Multi-fidelity near-optimal on-line control of a parallel hybrid electric vehicle powertrain”, *2019 IEEE Transportation Electrification Conference and Expo*, Novi, MI, USA, 19-21 June 2019.
26. P.G. Anselma, Y. Huo, J. Roeleveld, G. Belingardi, A. Emadi, “Integration of On-line Control in Optimal Design of Multimode Power-split Hybrid Electric Vehicle Powertrains”, *IEEE Transactions on Vehicular Technology*, vol. 68, no. 4, pp. 3436-3445, 2019.

Contact Information

Pier Giuseppe Anselma

Department of Mechanical and Aerospace Engineering (DIMEAS), Center for Automotive Research and Sustainable Mobility (CARS), Politecnico di Torino, Corso Duca degli Abruzzi 24, 10129 Torino, Italy.

Mail: pier.anselma@polito.it

Acknowledgments

This research was completed, in part, thanks to funding from the Canada Excellence Research Chairs (CERC) Program, Natural Sciences and Engineering Research Council of Canada (NSERC), Automotive Partnership Canada (APC) Initiative, along with the industrial partners FCA US LLC, and FCA Canada Inc.

This work is dedicated to the memory of Iman Aghabali and Mehdi Eshaghian.

Definitions/Abbreviations

CS	Charge-sustaining
DoF	Degree of freedom
DP	Dynamic programming
ECMS	Equivalent fuel consumption minimization strategy
EFC	Estimated fuel consumption
EPA	Environmental Protection Agency
eVT	Electrically variable transmission
FD	Final drive
HEV	Hybrid electric vehicle
HWFET	Highway fuel economy test
ICE	Internal combustion engine
MG	Motor/generator
OWC	One-way clutch
PEARS	Power-weighted efficiency analysis for rapid sizing
PG	Planetary gear
PMP	Pontryagin’s minimum principle
RWD	Real-world driving
SERCA	Slope-weighted energy-based rapid control analysis
SOC	State-of-charge
TG	Transfer gearset
UDDS	Urban dynamometer driving schedule
WLTP	Worldwide-harmonized Light-vehicle Test Procedure

Appendix

Table 5. Parameters of sizing candidates.

		Sizing options				
Sizing parameter	**Parameter**	**#1**	**#2**	**#3**	**#4**	**#5**
1) ICE	Displacement [L]	2.4	3.0	3.6	-	-
	Fuel (GS = gasoline ; DS = diesel oil)	GS	DS	GS	-	-
	Maximum power [kW]	132	166	189	-	-
	Maximum torque [Nm]	225	527	311	-	-
2) PG ratio (R:S)		2.65	3.15	4.15	-	-
3) MG2 TG ratio		2.09	2.59	3.59	-	-
4) Final drive ratio		3.09	3.59	4.09	-	-
5) MG1	Maximum power [kW]	10	20	35	45	60
	Maximum speed [rpm]	12500	14000	12000	14500	14500
	Maximum torque [Nm]	46	86	140	150	150
6) MG2	Maximum power [kW]	45	60	75	85	95
	Maximum speed [rpm]	14500	14500	14500	14500	14500
	Maximum torque [Nm]	150	150	180	315	344

Table 6. Parameters of identified optimal sizing candidates.

		Sizing options						
	Parameter	**eFlite®**	**OptGsl#1**	**OptGsl#2**	**OptGsl#3**	**OptDsl#1**	**OptDsl#2**	**OptDsl#3**
Data	ICE displacement [L]	3.6	3.6	3.6	3.6	3.0	3.0	3.0
	MG1 power [kW]	60	35	35	35	35	35	60
	MG1 power [kW]	85	95	85	95	85	95	85
	PG ratio	3.15	2.65	2.65	2.65	2.65	2.65	2.65
	MG2 TG ratio	2.59	2.09	2.59	2.09	2.09	2.59	2.59
	FD ratio	3.59	4.09	3.59	3.59	3.59	3.09	3.59
Fuel economy performance	EPA EFC [l/100 km]	8.35	7.92 (- 5.22 %)	8.16 (- 2.26 %)	7.67 (- 8.13 %)	4.81 (- 42.34 %)	5.28 (- 36.78 %)	4.79 (- 42.70 %)

	WLTP EFC [l/100 km]	15.27	14.56 (- 4.64 %)	14.04 (- 8.06 %)	13.81 (- 9.57 %)	9.33 (-38.40 %)	9.92 (-35.05 %)	9.41 (-38.38 %)
	RWD EFC [l/100 km]	6.35	6.68 (+ 5.04 %)	6.26 (- 1.45 %)	6.58 (+ 3.56 %)	4.25 (- 33.18 %)	4.69 (- 26.18 %)	4.28 (- 32.64 %)
Drivability performance	0-30 km/h time [s]	2.01	1.97	2.02	2.23	2.11	2.00	2.31
	30-60 km/h time [s]	1.93	1.92	1.94	1.95	1.91	1.92	1.95
	60-100 km/h time [s]	3.53	3.14	3.60	3.47	2.97	3.00	2.95
	100-130 km/h time [s]	3.58	3.14	3.64	3.45	2.45	2.95	2.85
	0-100 km/h time [s]	7.47	7.00 (- 6.29 %)	7.56 (+ 1.20 %)	7.65 (+ 2.41 %)	6.98 (- 6.56 %)	6.91 (- 7.50 %)	7.21 (- 3.48 %)